

# Efimov effect of triple stranded DNA: Real Space Renormalization Group and Zeros of partition function

Jaya Maji\* and Somendra M. Bhattacharjee†  
*Institute of Physics, Bhubaneswar-751005, India*  
 (Dated: July 17, 2012)

We study the melting of a three stranded DNA by using real space renormalization group and exact recursion relations. The prediction of an unusual Efimov-analog three chain bound state, that appears at the critical melting of a two chain DNA, is corroborated from the zeros of the partition function. The distribution of the zeros have been studied in detail for various situations. We show that the Efimov DNA can occur even if the three chain (*i. e.*, three monomer) interaction is repulsive in nature. In higher dimensions, a striking result that emerged in this repulsive zone is a continuous transition from the critical state to the Efimov DNA.

## I. INTRODUCTION

In recent times the formation of triple helical DNA has been a topic of considerable importance because of possible implications in the field of molecular biology. In 1957, it was discovered that certain sequences of Watson-Crick-double helical DNA allow a third strand DNA to bind via Hoogsteen or reverse Hoogsteen base pairing to form a triple helix[1–3]. This triple helix formation has the potentiality to block transcription and thereby affecting gene expression. Following this discovery the experimental demonstration of the ability of a third chain to recognize the base sequences without the double helical DNA revealing the base pairs, renewed the interest in triple helix DNA, especially its therapeutic applications[4, 5]. It is now known that not only DNA, even RNA[6] or PNA (polypeptide nucleic acid) are capable of forming triple helix with duplex DNA[7, 8].

A three stranded DNA has been shown to exhibit an Efimov like bound state near or at the critical melting of a duplex DNA[9]. The Efimov effect is the most striking phenomenon to occur in quantum three-body systems with only two-body short-range pair interactions[10–13]. An infinite number of bound states appear at the critical threshold of two body binding. There are several theoretical and experimental investigations using different models and methods to show this effect[14–17]. The universality of this phenomenon encompasses the analogous classical model, namely the melting of three stranded DNA[9]. The analogy is drawn between the large quantum fluctuations near the zero energy threshold of two body binding and the thermal Gaussian fluctuations at the melting of a duplex DNA. A scaling argument was used in Ref[9] to justify the occurrence of the effective two chain attractive potential  $\frac{1}{r^2}$  as a source of the Efimov effect. Such a long range interaction leads to a broad three-strand DNA bound state at or beyond the melting point of a duplex DNA. This is a state where no two are

bound but the three are bound together. Such a loosely bound state we called the Efimov-DNA. This has also been observed from the RG flows and the exact numerical calculations for several model systems, in particular on hierarchical lattices.

Hierarchical lattices, by virtue of their discrete scaling, allow one to solve many models in statistical mechanics by exact renormalization group (RG) transformations[18–21]. Furthermore many approximate real space RG on real lattices can be viewed as exact real space RG on hierarchical lattices. In the first study of the Efimov effect for Gaussian polymers, RG and exact numerics were used[9]. A part of our aim here is to analyze the Efimov phenomena exhibited by triple stranded DNA from the classical phase transition point of view, especially by looking at the zeros of the partition functions.

Finding the zeros of a partition function in the complex plane of any physical variable is a mathematical way to understand and analyze the phase transition phenomena. However finding those is often possible only for small sizes or soluble cases and not in general. Yang and Lee first studied the Ising Ferromagnetic system in a complex magnetic field to show that for a properly chosen variable the zeros lie on a unit circle, known as the Yang-Lee circle[22, 23]. Later the zeros were studied in the complex temperature plane and other variables[24]. Since there cannot be any real zero, the zeros may accumulate and pinch the real axis as a limit point in the thermodynamic limit. This limit point then identifies a transition point. This method can provide relevant information on phase transitions such as the critical field or temperature and the values of the associated critical exponents. Moreover, the distribution of zeros may form many complicated structures other than a circle. These structures are the separatrices of the two types of flows to the two different stable fixed points of the RG transformation, and are similar to the Julia sets (see appendix A)[25, 26].

In Ref[9] the RG flows were studied in the unbound region of the two and the three chain state. By looking at the flows in the unbound region of the duplex DNA, where chains are supposed to be free, an effective three chain bound state was predicted. In this paper we study

\*Electronic address: jayamaji@iopb.res.in

†Electronic address: somen@iopb.res.in

the partition function of the three chain system by combining the recursion relations and the RG transformations, and then finding the zeros. We also extend the model to the three chain repulsive interaction regime. In addition, we discuss several other features of the zeros in the complex plane, for instance the detail structure, and the connection to the Julia set.

This paper is organized as follows. In section II, the three polymer problem on a hierarchical lattice has been introduced. In section III, the recursion relations from RG decimation and those for exact iterations are written. The method of finding the zeros of the partition function is discussed and we find the limit point of the zeros to locate the phase transition. Section IV contains the results and discussions on the two and the three chain system under different situations. In particular we estimate the transition point for Efimov-DNA. Section V extends the problem to three chains repulsive interaction. The existence of a transition between the Efimov DNA and the critical repulsive state in higher dimensions is established there. Appendices A and B are for Julia set and limit cycle.

## II. MODEL

Let us consider the diamond hierarchical lattice as shown in Fig. 1. The lattice is generated iteratively by the replacement of each bond at the  $(n-1)^{\text{th}}$  generation by a motif of  $\lambda b$  bonds to get the  $n^{\text{th}}$  generation, where  $\lambda$  and  $b$  represent the bond scaling factor and the branching factor respectively. The thermodynamic limit is obtained by  $n \rightarrow \infty$  and in that limit the effective dimensionality of the lattice is

$$d = \frac{\ln \lambda b}{\ln \lambda}. \quad (1)$$

In this paper we shall choose  $\lambda = 2$ .

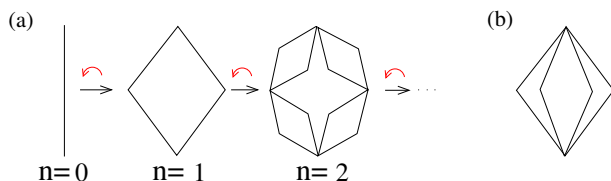


FIG. 1: (a) The recursive construction of the hierarchical lattice with  $b = 2$  for  $n = 0, 1, 2, \dots$  generations. The right arrows represent the direction of iteration towards larger lattices. The left arrows represent the direction of decimation used in RG. (b) A motif of  $2b$  bonds, where  $b = 4$ .

One major feature about hierarchical lattices is their unusual scale invariance property. They have a discrete scaling symmetry. That is why an exact implementation of the real space RG technique is possible. The decimation of the  $n^{\text{th}}$  generation to arrive at the  $(n-1)^{\text{th}}$  generation is precisely what is needed in an RG transformation. Once the partition function is known, it is

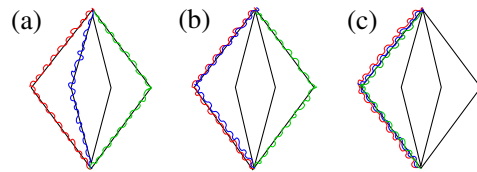


FIG. 2: Examples of three-chain configurations on a diamond motif for  $b = 4$ . (a) Polymers do not share any single bond. The number of such configurations is  $b(b-1)(b-2)$ . (b) Two polymers share a bond. The energy here is  $-2\epsilon$  and the number of such configurations is  $b(b-1)$ . (c) Three polymers share the same bond. The energy is  $2(-3\epsilon - \epsilon_{123})$ . The number of such configurations is  $b$ .

possible to calculate the free energy, and the other thermodynamic quantities. One may even write down recursion relations for them.

We consider three directed polymers on a diamond hierarchical lattice. Three chains on the diamond hierarchical lattice are stretched from bottom to top, but they can wander at intermediate points. The contact energies are defined at the bonds only. The polymers are assigned attractive potentials  $-\epsilon$  and  $-\epsilon_{123}$  ( $\epsilon, \epsilon_{123} > 0$ ) if a single bond is shared by the two and the three polymers respectively (see Fig. 2). At each generation, the length of each polymer increases by a factor  $\lambda = 2$  so that the length of polymers at the  $n^{\text{th}}$  generation is

$$L_n = 2^n. \quad (2)$$

For the Efimov effect, only pairwise interaction is enough. However in an RG procedure it is imperative to define the model with both  $\epsilon$  and  $\epsilon_{123}$ , because the three chain interaction gets generated on a longer scale.

## III. METHOD

### A. Renormalization Group

In this subsection we summarize the RG transformations and the exact recursion relations for the partition functions. The two ways of handling the problem are just two different ways to look at it. In the RG case, we start from a large lattice and remove short scale fluctuations by renormalizing the parameters, effectively reducing the size of the lattice. In contrast to this idea of thinning out the degrees of freedom, in the second method the lattice is built generation by generation so that one may study the behaviour of any quantity of interest as a function of length of the polymers. This is useful in studying phase transitions because finite size scaling can then be used to explore the nature of the transition.

We introduce the Boltzmann factors,

$$y = \exp(\beta\epsilon), \text{ and } w = \exp(\beta\epsilon_{123}), \quad (3)$$

where  $\beta = 1/k_B T$ ,  $k_B$  being the Boltzmann constant,  $T$  the temperature. The RG transformations of the two

chain and the three chain Boltzmann factors are given by

$$y' = \frac{(b-1) + y^2}{b}, \quad (4)$$

$$w' = \frac{(b-1)(b-2) + 3(b-1)y^2 + y^6 w^2}{b^2 y'^3}, \quad (5)$$

where the primed variables on the left hand side represent the renormalized values. These recursion relations show that the three body term is generated even-though we start with  $\epsilon_{123} = 0$ , *i. e.*,  $w = 1$ . As expected the three chain interaction does not affect (*i. e.*, renormalize) the two-chain interaction.

For a given  $y$  and  $w$ , the flows from successive use of Eqs. (4)-(5) would give us the phases and the nature of the transitions. One needs the fixed points for this analysis. For the two chain system, the fixed points of  $y$  are (i)  $y^* = \infty$  (stable zero temperature fixed point representing a bound duplex state), (ii)  $y^* = 1$  (stable infinite temperature fixed point representing an unbound state), and (iii)  $y^* = (b-1)$  (unstable fixed point representing the two chain melting or critical point). For pure three chain interaction ( $y = 1$ ) the fixed points of  $w$  correspond to (i)  $\infty$  (zero temperature), (ii) 1 (infinite temperature), (iii)  $(b^2 - 1)$  (unstable, three-chain critical point). The two chain melting is critical with a diverging length scale with exponent[18]

$$\nu = \frac{\log \lambda}{\log \left( \frac{dy'}{dy} \Big|_{y \rightarrow y_c} \right)} \quad (6)$$

and the specific heat exponent

$$\alpha = 2 - \nu. \quad (7)$$

At the two chain critical point  $y_c = b-1$ , the fixed point of  $w$  are found to be

$$w_{\pm} = \frac{b^2 \pm \sqrt{4 - 24b + 32b^2 - 12b^3 + b^4}}{2(b-1)^3}. \quad (8)$$

For  $b = 4$ ,  $w_{\pm} = \frac{8}{27} \pm i \frac{\sqrt{23}}{27}$ , are complex numbers. In the range  $3 \leq b < 8.56$  no real roots are found from the three chain RG relation (Eq. (5)). These complex roots lead to a limit cycle behaviour, which is intimately related to the Efimov effect (see appendix B).

### B. Exact recursion relations

With the trace over all configurations the  $n^{\text{th}}$  generation partition functions for single ( $C_n$ ), double ( $Z_n$ ) and triple ( $Q_n$ ) chain systems obey the recursion relations

$$C_n = b C_{n-1}^2, \quad (9)$$

$$Z_n = b(b-1)C_{n-1}^4 + b Z_{n-1}^2, \quad (10)$$

$$Q_n = b(b-1)(b-2)C_{n-1}^6 + 3b(b-1)C_{n-1}^2 Z_{n-1}^2 + b Q_{n-1}^2. \quad (11)$$

The initial conditions are taken as

$$C_0 = 1, Z_0 = y, Q_0 = y^3 w. \quad (12)$$

The average energy and the specific heat are defined as

$$E_n = \frac{\partial \ln Q_n}{\partial x}, \text{ and } C_n = \frac{\partial E_n}{\partial x}, \quad (13)$$

where  $x$  is the appropriate variable ( $y$  or  $w$  as the case may be). Though the definitions are different from the actual definitions, proportionality factors are not crucial here.

For given  $y$  and  $w$ , Eqs. (9)-(11) give the partition functions for different  $L_n$ . The average energy and the specific heat can be determined for different  $L_n$  by writing down the recursion relations for derivatives of Eqs. (9)-(11).

### C. Zeros of partition functions $Z_n, Q_n$

If we take  $w = 1$ , *i. e.*, no three body interaction, then the partition functions are polynomials in  $y$ . In general,  $Z_n$  is a polynomial in  $y$  of order  $L_n$  while  $Q_n$  is a multinomial in  $y$  and  $w$ . These partition functions are then completely described by the zeros, albeit complex. A phase transition is signaled by a real limit point of the zeros. However, the rapid growth of the order of the polynomials makes it difficult to implement this programme directly. A different representation is used to get the zeros[26].

By using the RG transformations of  $y$  and  $w$ , the recursion relations from Eqs. (9)-(11) can be reduced exactly to the forms

$$Z_n(y) = b^{L_n} Z_{n-1}(y'), \quad (14)$$

$$Q_n(y, w) = (b^{L_n})^{3/2} Q_{n-1}(y', w'), \quad (15)$$

with  $y', w'$  given by Eqs. (4), (5). These relations can be verified by direct substitution and, if necessary, by the method of induction.

Since the zeros determine a polynomial completely, the two chain partition functions can be written as

$$Z_n(y) = b^{L_n-1} \prod_{j=1}^{L_n} (y - q_j), \quad (16)$$

where  $q_j$ 's are the zeros of partition function  $Z_n(y)$ . These zeros appear in complex-conjugate pairs. With the substitution of  $Z_n(y)$ , Eq. (14) becomes

$$b^{L_n-1} \prod_{j=1}^{L_n} (y - q_j) = b^{L_n} b^{L_{n-1}-1} \prod_{j=1}^{L_{n-1}} (y' - \tilde{q}_j). \quad (17)$$

where  $\tilde{q}_j$ 's are the roots of  $Z_{n-1}$ . Then the use of Eq. (4) gives two roots from each factor on the right hand side, so that  $q_j$ 's are the solutions of

$$\frac{(b-1) + y^2}{b} = \tilde{q}_j, \quad (18)$$

*i. e.*,

$$q_j = \pm \sqrt{b\tilde{q}_j - (b-1)}. \quad (19)$$

It clearly shows that if we know the  $2^{n-1}$  zeros of  $Z_{n-1}(y)$ , we will be able to know the  $2^n$  zeros of  $Z_n(y)$ . One may start with the roots of  $Z_1$  and generate successively the roots of each generation, by just solving a quadratic equation.

Instead of generating all the roots, a random generation is more easily implementable. With an initial value  $y_0$  chosen randomly from the two roots of  $Z_1$ , the new roots are determined by Eq. (19). If one of them is chosen at random and substituted as  $\tilde{q}_j$ , the roots for the next generation can be found. Thus after the  $n^{\text{th}}$  iteration, the set obtained is basically the zeros in the complex  $y$ -plane. These roots are nothing but the zeros of partition function found from different sizes of the lattice, which in this problem would be equivalent to different lengths of polymers. The zeros quickly converge and as  $n \rightarrow \infty$  we look for the limit point on the real axis. Apart from that, the distribution in the complex  $y$ -plane itself is of interest. This method has been generalized for the three chain system.

#### IV. BEHAVIOR OF ZEROS: TWO CHAIN AND THREE CHAIN SYSTEMS

##### A. Two chain system: $b = 4$

For different branching factors, fractal like structures are obtained from the zeros of the partition functions of the two and the three chain systems. We considered only  $b = 4$  as a representative of the range where there are no real fixed point along the two chain critical line. For  $b = 4$

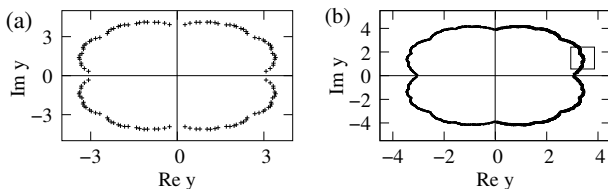


FIG. 3: Plot of zeros of  $Z_n(y)$  in the complex  $y$ -plane for  $b = 4$  from (a) exact recursion relation for  $n = 6$ , (b) RG relation. The closest point to the  $\text{Re}(y)$  axis approaches  $y_c = 3$ , the two chain melting point in the limit  $n \rightarrow \infty$ , the unstable fixed point of Eq. (4). The selected region shown by a box is zoomed in Fig. 4a.

the structure shown in Fig. 3a is obtained in the complex  $y$ -plane from the exact recursion relation Eq. (14). Exact solutions are possible only upto  $n = 6$  generation because of computational hardware limitations. This is insufficient, as thermodynamic limit ( $n \rightarrow \infty$ ) is needed to observe a phase transition. Finding zeros at random from the RG relations (Eqs. (4), (5)) wins over such difficulties and hence large lengths can be reached. The

zeros obtained from Eq. (18) give a fractal like structure shown in Fig. 3b. The accessed zero nearest to the real axis approaches the two chain transition point  $y_c = 3$  for large  $n$ . Apart from the limit point, the distribution of

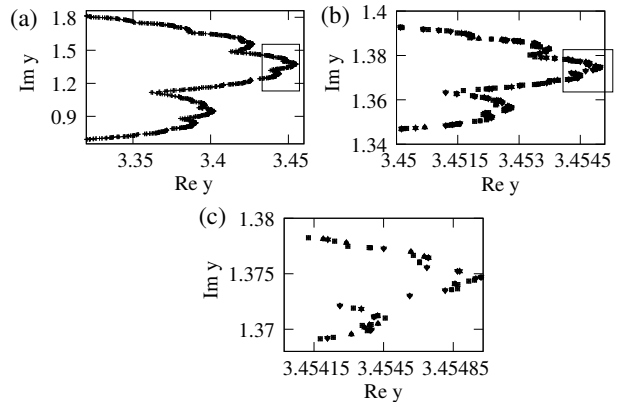


FIG. 4: Zeros of  $Z_n(y)$ : The inner rectangular box is zoomed successively. A self similar structure becomes apparent. Note that the zeros are known with high accuracy.

the zeros in the complex  $y$ -plane is also non-trivial.

The first feature to note is that the zeros do not seem to lie on a smooth differentiable curve. The zoomed picture of a small cross-section of the structure for the two chain system (from Fig. 3b) has been shown in Fig. 4a. Further the selected regions have been zoomed successively and are shown in Figs. 4b, 4c. The self similarity of the structure is visible. This is an indication of the fractal nature of the distribution. Further analysis required for a quantitative description is not done here.

These fractal like structures obtained above are nothing but the separatrices of the set of RG flows in the complex plane to the appropriate stable fixed points. These separatrices for iterations of any function in the complex plane are known as the Julia set (see appendix A). The sets are obtained after infinite number of iterations of a recursive formula by identifying the points that do not flow to the stable fixed points. Our method of finding the zeros by using the RG relations is in fact equivalent to an inverse iteration method, which is more efficient in producing such structures.

In Fig. 5a the RG flows are shown in the complex  $y$ -plane for a two chain system. The dotted line (red curve) is showing the flow towards the stable fixed point  $y = 1$ , *i. e.*, the high temperature region, when we start with a value from the inner region of the fractal like structure. On the other hand, a point from the outskirts of the line of zeros flows to the stable fixed point  $y = \infty$ , which is the bound state with zero temperature. The critical point being an unstable fixed point does not actually belong to the set but, as discussed, is a limit point — in a sense a boundary of the set.

The second feature to note is the 3-like shape near the real axis limit point. It is not arbitrary. The angle at the limit point in the complex plane is related to the specific

heat exponent by [27]

$$\tan(\phi\nu) = -\tan(\pi\alpha) + \frac{A_-}{A_+} \operatorname{cosec}(\pi\alpha), \quad (20)$$

where  $\phi$  is the angle between the tangent of zeros at the limit point, to the real axis of  $y$ , and  $A_{\pm}$  are the amplitudes of specific heat on the low and the high  $y$  side of the transition. Just like the exponents,  $A_-/A_+$  is a universal number for a universality class of transition. For the two chain problem, we know that  $A_-/A_+ \rightarrow \infty$  as  $A_+ = 0$ . Therefore the angle  $\phi$  is given by

$$\phi = \frac{\pi}{2\nu}. \quad (21)$$

The zeros obtained by the successive iterations of the

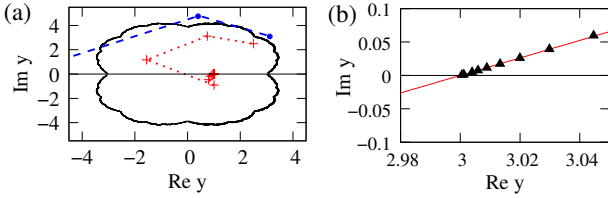


FIG. 5: (a) Plot of zeros of  $Z_n(y)$  in the complex  $y$ -plane. Two types of RG flows are shown. The dotted (red) curve starts from a point of the inner region and flows to  $y = 1$ . The dashed (blue) curve starts from a point of the outer region and flows to  $\infty$ . (b) The triangles are the zeros and approach the limit point  $y_c = 3$  at large  $n$ . The solid (red) line, given by Eq. (22) makes an angle  $\phi$  with the real axis with  $\nu$  of Eq. 6 and  $c = y_c$ .

one close to the real axis are shown in Fig. 5b by the triangles. They approach the real axis in a linear fashion with an angle  $\phi$ , given by the straight line

$$\operatorname{Im} z = (\operatorname{Re} z - c) \tan \frac{\pi}{2\nu}, \quad (22)$$

in generic complex  $z$  plane with  $\nu$  from Eq. (6). Here  $c$  represents the limit point of the zeros on the real axis. The zeros occur in complex conjugate pairs. Therefore if we take the mirror image of the distribution of zeros about the real axis in Fig. 5b, the beak of the 3-like shape can be obtained.

### B. Three chain system: $b = 4$

We have calculated the zeros of  $Q_n(1, w)$  for a three chain system with a pure three chain interaction. By considering  $y = 1$  in Eq. (5), we get

$$w' = \frac{(b^2 - 1) + w^2}{b^2}. \quad (23)$$

The zeros come from the equation

$$\tilde{q}_j = \pm \sqrt{b^2 \tilde{q}_j - (b^2 - 1)},$$

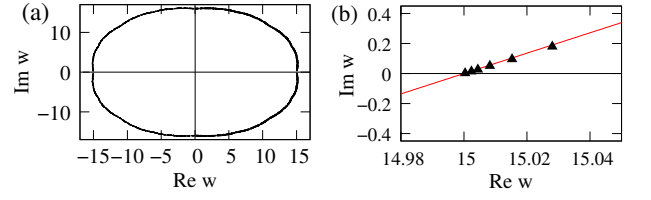


FIG. 6: (a) Plot of the zeros of  $Q_n(1, w)$  in the complex  $w$ -plane for  $b = 4$ . The closest point to the real axis approaches  $w_c = 15$  for large  $n$ . There is self similarity in the distribution of zeros, but not shown here. (b) The triangles are the zeros. The solid (red) line given by Eq. (22) passes through them with  $\nu$  of Eq. (27) and  $c = w_c$ .

where  $\tilde{q}_j$ ,  $q_j$ 's are the zeros of  $Q_{n-1}(1, w)$  and  $Q_n(1, w)$  respectively. The distribution of zeros is the Julia set give the fractal like structure shown in Fig. 6a. By choosing the zero near to the limit point  $w_c$ , the nature of the distribution can be determined as shown in Fig. 6b by the straight line given by Eq. (22) with  $\nu$  of Eq. 27 and  $c = w_c$ .

### C. Efimov DNA: $b = 4$

The idea is to show the Efimov transition point of DNA by finding the limit point of zeros on the real  $y$  axis. Although we consider  $w = 1$ , the effective three chain interaction develops by renormalization. As a result the zeros found from Eqs. (9)-(11) seem to pinch the  $\operatorname{Re}(y)$  axis at a point where none of the pair is bound. The exact solutions are shown in Fig. 7a for  $n = 6$ . On a more finer scale the zeros are shown in Fig. 7b. For such small lattices the limit point is not accessible, hence an extrapolation scheme may be used. The zeros nearest to the  $\operatorname{Re}(y)$  axis, obtained in different generations ( $n = 2, \dots, 6$ ) are shown in Fig. 7c by black dots. A straight line nicely fits these zeros, and is shown by a solid (red) curve.

The straight line intersects the real axis at  $y = 2.321$ . This value is the large  $n$  extrapolation and can be taken as the estimate of the Efimov transition. We may compare this extrapolated value with the previous RG based estimate of  $y_E = 2.32402$ . Finding the zeros for two chain system is easier than for the three chain system. Since the three chain equation holds both the variables  $y, w$ , finding zeros from the three chain RG relation is tantamount to generating the full relation for  $Q_n$ . This is because one needs to keep  $w$  at all the intermediate values of  $n$  and then at the end of the desired value of  $n$ ,  $w$  is to be set to 1. One sees the difficulty of the Efimov physics eventhough  $w = 1$ . It is tempting to simplify the recursion relation at the cost of some approximation. We set  $w = w' = 1$  to get a renormalized  $y'$  that would describe the three chain system. Such a relation follows

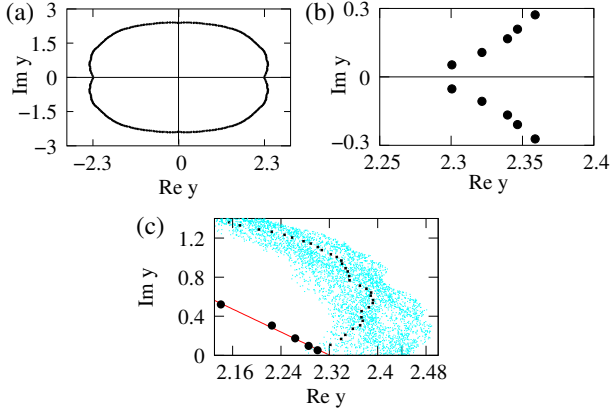


FIG. 7: Plot of zeros in the complex  $y$ -plane for  $b = 4$ . (a) Zeros of  $Q_n(y, 1)$ , when  $n = 6$ , (b) a finer scale of (a) near the real axis, (c) Combined plot of zeros. The bigger black circles are the zeros closest to the real axis (*i. e.*, with smallest imaginary part) obtained from  $Q_n(y, 1)$  for  $n = 2, \dots, 6$  and the solid straight line is a fit to these. The shaded regime shows the distribution of zeros (from Eq. 24) on which we superpose the positive quadrant of (a) shown by the small black dots.

from Eq. (5), as

$$y'^3 = \frac{(b-1)(b-2) + 3(b-1)y^2 + y^6}{b^2}. \quad (24)$$

The zeros obtained from Eq. (24) spread out in a “milky way” over a region in the complex plane of  $y$ . The spread makes it difficult to make an estimate of the real axis limit point, but one may use the width to put a bound on the Efimov transition point (see Fig. 7c).

#### D. Efimov DNA at $y_c = b - 1$ : $b = 9$

The study along the critical threshold of the two chain melting is quite interesting. No real fixed point for  $w$  exists for Eq. (5) when  $b$  is in the range  $3 \leq b \leq 8.56$  along the  $y = y_c$  line. For  $y = y_c$ , the single parameter RG relation is

$$w' = \frac{(b-2) + 3(b-1)^2 + (b-1)^5 w^2}{b^2(b-1)^2}. \quad (25)$$

The two fixed points for this case are given by Eq. (8). For  $b = 9$ , these are

$$w = w_s = 0.0655347.. \quad (\text{stable}), \quad (26a)$$

$$w = w_E = 0.0926684.. \quad (\text{unstable}). \quad (26b)$$

The unstable fixed point as the phase transition point, determines the limit point of the zeros of the partition function on the real axis. Hence it can be predicted that at the two chain melting point, by tuning  $w$ , a transition

occurs at  $w = w_E$ , from the Efimov DNA to the critical state of polymer pairs. Fig. 8a shows the distribution of zeros of  $Q_n(y_c, w)$  in the complex  $w$  plane. The set of these zeros is a Julia set, separating the flows to the stable fixed points. The stable fixed point in the inner region of the set is given by Eq. (26a). The zeros near the real axis approach  $w = w_E$  linearly, following Eq. (22) with  $c = w_E$  and  $\nu$  of Eq. (28) as shown in Fig. 8b. A detailed discussion is given in the next section.

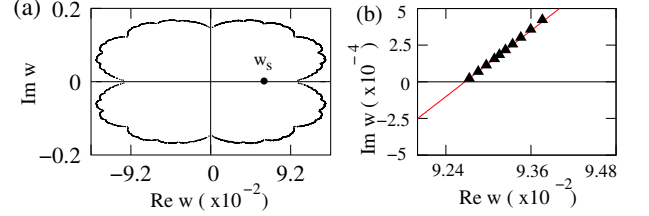


FIG. 8: (a) Zeros of  $Q_n(y_c, w)$  in the complex  $w$ -plane for  $b = 9$ . The stable fixed point  $w = w_s$  is shown by a black circle. (b) The solid (red) line is given by Eq. (22) and passes through the zeros shown by the triangles, with  $\nu$  from Eq. (28) and  $c = w_E$ .

## V. EFIMOV DNA: RG FLOW AND NUMERICAL EVIDENCE

To explore the robustness of the Efimov effect, we now include a three chain repulsive interaction along with the pairwise attractive one. The three chain interaction is attractive when  $w > 1$  and repulsive for  $0 \leq w < 1$ . For  $w = 0$ , representing the hard core three chain repulsive interaction, three chains can never be on the same bond in this model.

### 1. $b = 4$

For  $b = 4$  the RG phase diagram is shown in Fig. 9a. The solid (red) line is the separatrix connecting the pure three chain transition point  $(1, w_c)$  to an Efimov transition point for  $w = 0$ . Each point on the solid line represents the Efimov transition point. In other words keeping  $w$  fixed, by changing  $y$ , we would see a melting of a loosely bound Efimov DNA with no pairwise binding. The region enclosed between this separatrix (solid red line) and the  $y_c = 3$  line is the Efimov region and  $(y, w)$  flows to  $(1, \infty)$ . Below the solid (red) line is the high temperature zone of denatured DNA, where RG flows are to  $(1, 1)$ . The region right to the  $y_c = 3$  line is the two chain bound state. The area below the dashed curve where the RG flow takes  $w$  to zero when two chain pairs are strongly bound, represents a different state where one finds a three chain bound state but with no three chain contact. The dashed line is then a crossover line. It remains to be seen if under some conditions this crossover



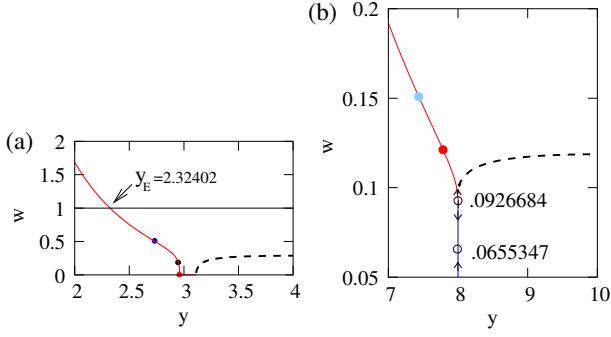


FIG. 9: RG phase diagram in the  $y$ - $w$  plane. (a) For  $b=4$ . The solid (red) curve and the dashed curve represent the separatrices, where  $w$  flows to two different fixed points on either side of the separator. For  $w = 1$ ,  $y_E = 2.32402$  is the Efimov-DNA transition point. The filled circles are the Efimov transition points for  $w = 0.5$ ,  $w = 0.2$ ,  $w = 0$  respectively, obtained from Fig. 10a. (b) For  $b=9$ . Along  $y_c = 8$ , there are two real fixed points given by Eq. (26a). Solid (red) and dashed lines are the separatrices. The filled circles are the Efimov transition points for  $w = 0.15$  and  $w = 0.12$  respectively, obtained from Fig. 10b.

line becomes a true phase transition line.

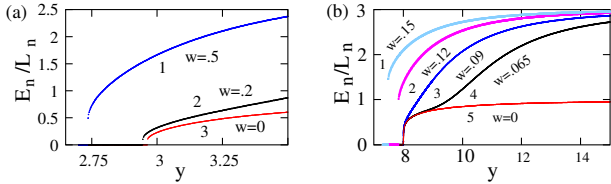


FIG. 10: The three chain average energy per monomer with  $y$  from direct computation. (a) For  $b = 4$ , the average energy curves (marked 1, 2, 3) with the fixed values  $w = 0.5$ ,  $w = 0.2$ ,  $w = 0$  show first order transitions. (b) For  $b = 9$ , the average energy curves (marked 1, 2) with the fixed values  $w = 0.15$ ,  $w = 0.12$  show first order transitions. Curves (marked 3, 4, 5) with the constant values  $w = 0.09$ ,  $w = 0.065$ ,  $w = 0$  show a continuous transition at  $y_c = 8$ .

$$2. \quad b = 9, y_c = b - 1$$

The RG phase diagram is shown in the Fig. 9b for  $b = 9$ . In the diagram two separatrices (solid and dashed) meet at an unstable fixed point. The two fixed points  $w = w_s$  and  $w = w_E$  are shown in Fig. 9b. The presence of any unstable fixed point reflects a continuous transition along the two chain critical line. Hence we can say that by tuning the three chain repulsive interaction parameter or temperature in the repulsive zone a transition can be induced in the Efimov DNA at the critical threshold of duplex binding. The transition is from the Efimov state to the critical state of pairs dominated by the three chain repulsion. The Efimov region is now restricted by a separatrix connecting the two unstable fixed

points  $(1, w_c)$  and  $(y_c, w_E)$  and the critical line  $y_c = b - 1$ .

On the critical line at both the fixed points  $w = w_s$  and  $w = w_E$ ,  $y$  is a relevant variable (unstable in the  $y$  direction). But  $y$  does not couple to  $w$  in the RG equation (Eq. (4)). The melting for  $w < w_E$  would be similar to the pure two chain melting described by Eqs. (6), (7). In the  $y$ - $w$  plane,  $(y_c, w_E)$  is a multicritical point where the line of first order transitions goes over to a line of critical points.

### 3. Data collapse

We now provide numerical evidences for the above RG-based inferences. The exact numerical calculations of the average energy and the specific heat by iterating the partition functions and their higher derivatives for lattices of various sizes are done for different fixed values of  $w$ . Fig. 10a for  $b = 4$  shows that at  $w = 0.5$ ,  $w = 0.2$  and  $w = 0$ , there are first order transitions. The transition points estimated from the point of discontinuity are shown by the filled circles in Fig. 9a. They are on the separatrix, and are the Efimov transition points for the corresponding values of  $w$ .

The energy curves in Fig. 10b for  $b = 9$  with  $w = 0.15$  and  $w = 0.12$ , show first order transitions. These transition points are shown by the filled circles in Fig. 9b. In contrast, the energy curves (marked 3, 4, 5) show continuous transitions for  $w = 0.09$ ,  $w = 0.065$ ,  $w = 0$  respectively at  $y_c = 8$ . This is consistent with the RG prediction of Fig. 9b.

The energy and the specific heat curves are shown in Figs. 11a, 11b for  $b = 9$ ,  $y = 1$  and in Figs. 12a, 12b for  $b = 9$ ,  $y_c = b - 1$ . Also corresponding finite size scaling are shown in Figs. 11c, 11d for  $b = 9$ ,  $y = 1$  and in Figs. 12c, 12d for  $b = 9$ ,  $y_c = b - 1$ . Finite size scaling behavior of different thermodynamic quantities are described by the length scale exponents. In analogy with the Eq. (6), the exponent to describe the three chain transition for  $y = 1$  and  $y_c = b - 1$  at appropriate critical points are given by,

$$\nu = \frac{\log 2}{\log \frac{2(b^2-1)}{b^2}}, \quad (27)$$

$$\nu = \frac{\log 2}{\log \left( \frac{\partial w'}{\partial w} \Big|_{y_c=b-1, w \rightarrow w_E} \right)}. \quad (28)$$

Around a critical point one should see a finite size scaling. Therefore the average energy and the specific heat obeying the finite size scaling can be written in the forms

$$E \sim L^{1/\nu} f(L^{1/\nu} |w - w^*|), \quad (29)$$

$$C \sim L^{2/\nu} f(L^{1/\nu} |w - w^*|), \quad (30)$$

with appropriate  $\nu$  and  $w^*$ . In Figs. 11c, 11d we see that the average energy and the specific heat scaled as  $E_n L_n^{-1/\nu}$  and  $C_n L_n^{-2/\nu}$  respectively, when plotted with

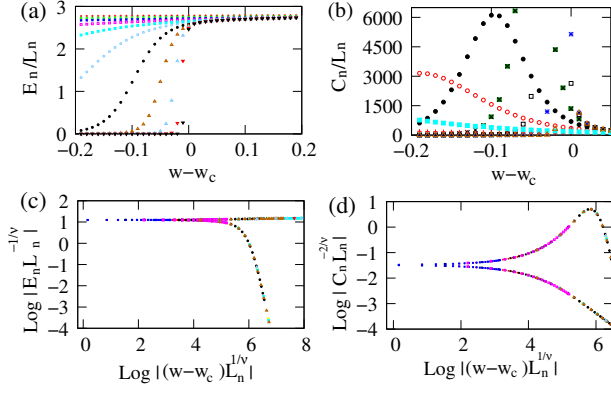


FIG. 11: (a) For  $b=4$ . (a) The three chain average energy per monomer versus the corresponding Boltzmann factor for chain length upto  $2^{26}$  when  $y = 1$ . The average energy shows a continuous transition at the  $w = w_c$ . (b) The three chain specific heat ( $C_n$ ) per monomer with the corresponding Boltzmann factor. (c) Data collapse of energy. (d) Data collapse of specific heat.

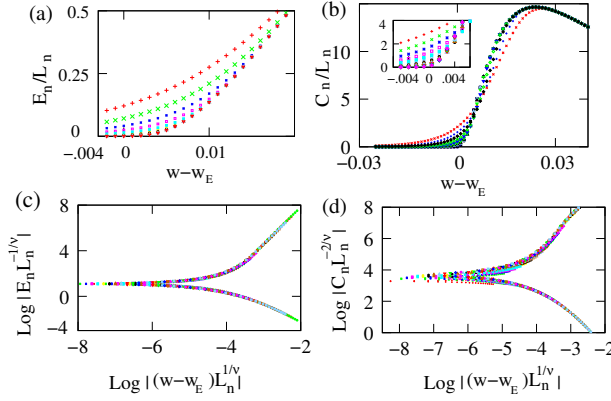


FIG. 12: For  $b=9$ . (a) The three chain average energy per monomer versus the corresponding Boltzmann factor for chain length upto  $2^{26}$  when  $y_c = b - 1$ . The average energy shows a continuous transition at  $w = w_E$ . (b) The three chain specific heat ( $C_n$ ) per monomer with the corresponding Boltzmann factor. Length dependence is shown in the inset. (c) Data collapse of energy. (d) Data collapse of specific heat.

$|(w - w^*)|L_n^{1/\nu}$  with the  $\nu$  of Eq. (27) and  $w^* = w_c$  for  $y = 1$ , all the data collapse on a single curve for different lengths of polymers, where  $n = 6, 7, \dots, 26$ .

Figs. 12c, 12d show similar plots for the critical line ( $y_c = b - 1$ ) with  $\nu$  of Eq. (28) and  $w^* = w_E$ . Since the specific heat diverges with increasing length, data collapse is good for the case  $y = 1$ . The data collapse for the case  $y_c = b - 1$  is not so good due to a smoother behavior of specific heat at the critical point. These establish the weak criticality at  $w = w_E$ .

## VI. SUMMARY

To summarize, the RG relations and exact recursion relations are used to study the three chain system on a diamond hierarchical lattice. Our emphasis is on the Efimov like state exhibited by the three chain system at or beyond the two chain melting, where no two are bound, and the nature of transitions. Fractal like structures are obtained for the zeros of the partition functions. These zeros when they pinch the real axis, determine the phase transition points. We find that all the transition points obtained from RG flows, are in good agreement with the zeros of partition function on the real axis. The Efimov transition point thus found strengthens the prediction of the Efimov like phenomena for the three chain system. We have shown that the Efimov effect is exhibited by a three chain system even if there is a repulsive three chain interaction. A transition can be induced in higher dimensions from the Efimov state to the three chain critical repulsive state at the melting of a duplex DNA. The transition to this three chain critical repulsive state is continuous and obeys the finite size scaling law with exponents obtained from RG. In the  $(y, w)$  phase diagram,  $(y_c, w_E)$  is a multicritical point.

We await experimental evidences for the existence of the Efimov DNA. Calorimetric experiments looking for the thermodynamic signatures of the Efimov transition would be as effective as finding the structure of DNA. Again the existence of such a state remains a challenge for molecular dynamics and Monte Carlo simulations.

## Acknowledgments

JM would like to thank Professor A. Khare for discussions on Julia sets.

## Appendix A: Julia set

The standard definition of a Julia set is the set of points on the complex plane which flow to a fixed point (no divergence) after a function, *e. g.*,

$$z_n = z_{n-1}^2 + c, \quad (\text{A1})$$

is repeatedly applied, where  $c$  is any arbitrary constant, and could be real or complex. Let us choose  $c = 0$ . The fixed point solution for  $c = 0$  are  $z = 0, 1, \infty$ , where  $z = 1$  is the unstable fixed point. Here for  $n \rightarrow \infty$ ,  $z_{n+1} \rightarrow 0$ , when starting with  $|z_0| < 1$  and  $z_{n+1} \rightarrow \infty$ , when starting with  $|z_0| > 1$ . Therefore the unit circle  $|z| = 1$  is the boundary between the two stable fixed points  $z = 0, \infty$ . The unstable point lies on this boundary.



## Appendix B: Limit Cycle

For two successive generations Eqs. (5) will be

$$w_n - w_{n+1} = f(w_{n+1}) - w_{n+1}. \quad (\text{B1})$$

But if the continuum limit is taken, Eq. (B1) can be written as

$$l \frac{dw}{dl} = -(w - w_+)(w - w_-), \quad (\text{B2})$$

at the critical line  $y_c = b - 1$ , where  $l = \ln L$  and  $L = 2^n$ . For complex  $w_{\pm} = \alpha \pm i\beta$ , the solution of Eq. (B2) is then

$$w = \alpha - \beta \tan \beta (\ln l + \theta), \quad (\text{B3})$$

where  $\theta$  is the integration constant. The above equation reflects the periodicity of  $w$  in  $\ln l$  with the property

$$w(l) = w(l\lambda), \text{ where } \ln \lambda = \frac{\pi}{\beta}. \quad (\text{B4})$$

Here as  $l$  increases  $w$  approaches  $\pm\infty$ . This behavior can be mapped into a limit cycle in the complex plane with a phase factor defined by the equation

$$e^{i\phi} = \frac{w - w_+}{w - w_-}. \quad (\text{B5})$$

With the help of Eq. (B2) and its derivative,  $\phi$  will be

$$\phi = \frac{\beta}{\alpha} \ln l + \phi_0, \quad (\text{B6})$$

where  $\phi_0$  is the integration constant.

Our model on the hierarchical lattice is a discrete model. Certainly a limit cycle is obtainable from the RG relations in the continuum limit, but it is not straight forward to do so in the discrete case.

- 
- [1] G. Felsenfeld, D. R. Davies, A. Rich, J. Am. Chem. Soc. **79**, 2023 (1957).
  - [2] H. E. Moser, P. B. Dervan, Science **238**, 645 (1987).
  - [3] T. Le Doan *et al*, Nucleic Acids Res. **15**, 7749 (1987).
  - [4] A. Jain *et al*, Biochimie **90**, 1117 (2008); M. Duca *et al*, Nucleic Acids Res. **36**, 5123 (2008).
  - [5] Michael M. Seidman, Peter M. Glazer, J. Clin. Invest., **112**, 487 (2003).
  - [6] R. W. Roberts and D. M. Crothers, Science **258**, 1463 (1992).
  - [7] P. E. Nielsen, Ann. Rev. Biophys. Biomol. Struct. **24**, 167 (1995).
  - [8] L. Betts *et al*, Science **270**, 1838 (1995).
  - [9] Jaya Maji, S. M. Bhattacharjee, F. Seno, A. Trovato, New J. Phys. **12** (2010) 083057.
  - [10] V. Efimov, Phys. Letts. **B 33**, 563 (1970).
  - [11] V. Efimov, Yad. Fiz. **12**, 1080 (1970); Sov. J. Nucl. Phys. **12**, 589 (1971).
  - [12] V. Efimov, Sov. J. Nucl. Phys. **29**, 546 (1979).
  - [13] A. C. Fonseca, E. F. Redish, P. E. Shanley, Nuc. Phys. **A 320**, 273 (1979).
  - [14] M. Zaccanti *et al*, Nature Physics **5**, 586 (2009).
  - [15] T. Kraemer *et al*, Nature **440**, 315 (2006).
  - [16] D. V. Fedorov, A. S. Jensen, K. Riisager, Phys. Rev. Lett. **73**, 2817 (1994).
  - [17] E. Braaten, H. W. Hammer, Phys. Rept. **428**, 259 (2006).
  - [18] S. Mukherji, S. M. Bhattacharjee, Phys. Rev. **E 52**, 1930 (1995).
  - [19] M. Kaufman, R. B. Griffiths, Phys. Rev. **B 24**, 496 (1981).
  - [20] T. A. S. Haddad, S. R. Salinas, Physica **A 306**, 98 (2002); T. A. S. Haddad, R. F. S. Andrade, S. R. Salinas, J. Phys. A: Math. Gen. **37** 1499 (2004).
  - [21] M. Hinczewski, A. N. Berker, Phys. Rev. **E 73**, 066126 (2006).
  - [22] C. N. Yang, T. D. Lee, Phys. Rev. **87**, 404 (1952).
  - [23] T. D. Lee, C. N. Yang, Phys. Rev. **87**, 410 (1952).
  - [24] M. E. Fisher, in *Lectures in Theoretical Physics*, vol. **7**, (University of Colorado, Boulder, 1965).
  - [25] G. Julia, J. Math. Pures Appl. **4**, 47 (1918).
  - [26] B. Derrida, L. De Seze, C. Itzykson, J. Stat. Phys. **33**, 3 (1983).
  - [27] C. Itzykson, R. B. Pearson, J. B. Zuber, Nuclear Phys. **B 220**, 415 (1983).